Full Paper

Rikkunshito, a Kampo Medicine, Ameliorates Post-operative Ileus by Anti-inflammatory Action

Mari Endo[1], Masatoshi Hori[2,*a], Hiroshi Ozaki[2], Tetsuro Oikawa[1,*b], and Toshihiko Hanawa[1,3]

[1]*Department of Clinical Research, Oriental Medicine Research Center, Kitasato University, Tokyo 108-8642, Japan*
[2]*Department of Veterinary Pharmacology, Graduate School of Agriculture and Life Sciences, The University of Tokyo, Tokyo 113-8657, Japan*
[3]*Kitasato University Graduate School, Doctoral Program of Medical Science, Oriental Medicine, Tokyo 108-8642, Japan*

Abstract. Rikkunshito (RKT), a Kampo (Japanese herbal) medicine, is used as a prokinetic for patients with various diseases including functional dyspepsia. RKT promotes delayed gastric emptying via 5-HT$_3$ receptor blockade. Otherwise, RKT increases ghrelin release via 5-HT$_{2B}$ and 5-HT$_{2C}$ receptor activation. Recent studies revealed that ghrelin and 5-HT$_3$ receptor antagonists have an anti-inflammatory effect. So we hypothesize that RKT may have an anti-inflammatory action in the post-operative ileus. Intestinal manipulation (IM) was applied to the distal ileum of mice. RKT was administered orally 4 times before and after IM. Gastrointestinal transit in vivo, leukocyte infiltration, and gastric emptying were analyzed. We also investigated the effects of the 5-HT$_3$ receptor agonist *m*-chlorophenylbiguamide (mCPBG) and ghrelin-receptor antagonist [D-Lys3]-GHRP-6 on the ameliorative action of RKT. RKT treatment led to recovery of the delayed intestinal transit and gastric emptying rate induced by IM. RKT significantly inhibited the infiltration of neutrophils and macrophages. [D-Lys3]-GHRP-6 reduced and mCPBG partially reduced the RKT-mediated anti-inflammatory activity, as monitored by infiltrating macrophages and neutrophils. RKT serves as a novel therapeutic agent for POI characterized by its anti-inflammatory potency, in addition to prokinetic action. The RKT-induced anti-inflammatory activity may be partly mediated by inhibition of the 5-HT$_3$ receptor and ghrelin release.

Keywords: anti-inflammatory action, rikkunshito, postoperative ileus, ghrelin, 5-HT$_3$

Introduction

Rikkunshito (RKT) is a Kampo (Japanese herbal) medicine and is known as a prokinetic agent for patients with various diseases such as functional dyspepsia (1). RKT promotes delayed gastric emptying through antagonistic action against the 5-HT$_3$ receptor (2). RKT is also known as a prescription to increase appetite, and its action mechanisms were mediated from inhibition of 5-HT$_{2B}$ and 5-HT$_{2C}$ receptors (3). Activation of 5-HT$_{2B}$ and 5-HT$_{2C}$ receptors inhibits ghrelin secretion (3), in other words, inhibition of these receptors enhances ghrelin secretion indirectly. Furthermore, recent study has also revealed that gentle cecal manipulation between two fingers for 1 min (abdominal surgery) induced rapid inhibition of circulating acyl ghrelin in rats (4). Administration of ghrelin stimulates gastric motility, with increased gastric tone and emptying, and also increases activity of migration motor complexes in the small bowel (5 – 7). On the other hand, 5-HT$_3$ receptor antagonists granisetron and tropisetron or ghrelin were reported to ameliorate inflammation of colitis (8, 9). Taken together, RKT might have both prokinetic and anti-inflammatory action. This possibility finally led us to the hypothesis that RKT shows anti-inflammatory activity on postoperative ileus (POI), which is characterized by gastrointestinal motility dysfunction and inflammation in the gastrointes-

tinal muscle layer (10 – 12).

The present investigation was made to clarify the anti-inflammatory activity of RKT, using a mouse POI model.

Materials and Methods

Animals

Male BALB/c mice (Japan SLC, Hamamatsu) weighing 21 – 26 g (6 – 7-week-old) were used. Mice were housed by 1 or 2 individuals per cage under conditions of constant temperature ($23°C \pm 2°C$) and humidity ($55\% \pm 10\%$) with standard rodent chow and water ad libitum and a 12-h light/dark cycle. All animal experiments were performed according to the "Regulations for the Care and Use of Laboratory Animals in Kitasato University", published by Kitasato University. The Institutional Animal Care and Use Committee for Kitasato University approved the study protocol.

Preparation of Kampo medicines

RKT was blended in the Oriental Medicine Research Center of Kitasato University. Daily human doses of the crude herbs (ninjin, *Ginsenradix* 4.0 g; byakujyutu, *Atractylodisrhizoma* 4.0 g; bukuryo, *Hoelen* 4.0 g; hange, *Pinelliaetuber* 4.0 g; chimpi, *Aurantiinobilispericarpium* 2.0 g; taiso, *Zizyphifructus* 2.0 g; kanzo, *Glycyrrhizaeradix* 1.0 g; shokyo, *Zingiberisrhizoma* 0.5 g) in RKT were decocted with 600 ml of distilled water until the filtered decoction was reduced by half. The decocted extract solution was centrifuged at 3,000 rpm for 15 min, and the supernatant was lyophilized. The obtained freeze-dried powder (5.65 g) was dissolved in distilled water to the appropriate dose just before administration. In the current series of experiments using mice, the daily human dose (113 mg/kg) was used.

Three-dimensional HPLC

RKT was dissolved with H_2O, and then the filtered material was analyzed by HPLC (ACQUITY UPLC; Nihon Waters K.K., Tokyo) under the following conditions: the sample (10 μl) was applied to a COSMOSIL C18-MS-II column (3.0 × 50 mm; Nacalai Tesque, Inc., Kyoto). The mobile phase was water (H_2O)/acetonitrile (CH_3Hn) (9:1) for the first 10 min, changing to a linear gradient of (1:1) over 85 min. The flow rate was 1.0 ml/min and the oven temperature was 30°C. HPLC patterns were analyzed by absorbance at 200 – 340 nm.

Intestinal manipulation (IM) for mouse model of POI

All animals were anesthetized with isoflurane (Escain; Mylan, Inc., Tokyo) or pentobarbital sodium (Somnopentyl; Kyoritsu Seiyaku Corp., Tokyo). IM was performed as reported previously (13, 14). Briefly, the distal ileal part (10 cm from the ileocecal valve) was exteriorized and then gently scraped with compression along its entire length for about 3 – 5 min at a strength equal to general writing pressure using a sterile cotton applicator moistened with physiological saline. After manipulation, the abdomen was closed with sutures.

Intestinal transit determination

Twenty-three hours after IM with fasting, the non-absorbable marker, 80 μl of 0.25% (w/v) phenol red (PR) in phosphate buffered saline (PBS), was orally administered to mice via a gastric tube. After 1 h, the gastrointestinal part was isolated and the stomach and intestine were separated as a single stomach segment (Sto), ten small intestine segments (SI1-SI10), a single cecum segment (Cec), and three colon segments (Co1-Co3). The contents of each segment were mixed with 0.1 N sodium hydroxide. Proteins in the sample were precipitated by addition of 20% (w/v) trichloroacetate. The optical density volume of each supernatant after centrifugation at $1600 \times g$ for 20 min with 0.6 N sodium hydroxide was then determined at 570 nm. The volume of PR for 15 segments was calculated using a standard curve. Each geometric center (GC) of distribution for PR in 15 segments of the gastrointestinal tract was calculated using the following formula (10, 14): GC = Σ {(% of each fluorescence signal) × (segment number)} ÷ 100.

Gastric emptying rate by ^{13}C-acetate breath test

Twenty-three hours after IM with fasting, mice were given [1-^{13}C] sodium acetate (Cambridge Isotope Laboratories, Woburn, MA, USA)-labeled solid test meal and placed in test chambers. To collect air from the chambers, we used the noninvasive breath test system (15), comprising 4 animal chambers, a pump, and breath sampling bags. Expired air was collected and measured at 5-min intervals until 30 min, with additional measurements at 10-min intervals until 60 min. $^{13}CO_2$ levels in the trapped air were measured by POC one (Ohtsuka Electronics Co., Ltd., Tokyo) and are given as $\Delta^{13}CO_2$ (‰), as reported previously (16).

Whole-mount preparations

Histochemical examination was performed on whole-mount muscular preparations of the ileum. Whole-mount muscular (5 cm from ileocecal valve of the distal ileal region) samples were prepared as reported previously (15, 17, 18). Mucosa-free muscular whole mounts were fixed in 4% paraformaldehyde in PBS for 30 min at 4°C. After fixation, whole mounts were washed in PBS and were then cut and used for staining procedures.

Whole-mount histochemistry and immunohistochemistry

Muscular whole-mount preparations were used for immunohistochemical analysis of CD68 and PGP9.5. Each whole mount preparation was incubated with 0.2% Triton X-100 in PBS at room temperature (RT) for 2 h. After blocking with 2% BSA in PBS at RT for 1 h, the preparations were incubated overnight with primary antibody (rat anti-mouse CD68 Ab, dilution 1:1000; Serotec, Düsseldorf, Germany; and rabbit anti-human PGP9.5 poly Ab, dilution 1:1000; Cosmo Bio Co., Ltd., Tokyo) at 4°C. Then the preparation was washed 3 times in PBS, incubated in 5% normal donkey and goat IgG in blocking buffer for 15 min, followed by the appropriate secondary antibody (donkey anti-rat Alexa 488, dilution 1:500; Molecular Probes Inc., Eugene, OR, USA; and goat anti-rabbit Alexa 568, dilution 1:500; Invitrogen, Carlsbad, CA, USA) at RT for 90 min. After washing 3 times, the preparations were cover-slipped and inspected by confocal microscopy (ECLIPSE Ti; Nikon, Tokyo) or fluorescence microscopy (BX41; Olympus Corporation, Tokyo). CD68-positive cells were counted in 3 randomly selected fields in each specimen of 0.1024 mm^2 by confocal microscopy or 0.0825 mm^2 by fluorescence microscopy. The same experiment was performed 4 times in order to calculate means ± S.E.M.

In order to detect myeloperoxidase (MPO)-positive neutrophils, freshly prepared whole-mount preparations were histochemically stained with PBS containing 0.1% (w/v) Hanker-Yates reagent (Polysciences, Warrington, PA, USA) and 0.03% (v/v) hydrogen peroxidase (Wako Pure Chemical Industries, Ltd., Osaka) and then rinsed in PBS (19). Cells that were obviously MPO-positive in the muscularis were counted under a microscope (BX41; Olympus Corporation) in 3 randomly selected fields for each specimen of 0.0825 mm^2.

Experimental design

Animals were randomly divided into the following experimental groups: 1) Normal, no treatment, no IM; 2) Control (IM + vehicle), ultrapure water was orally administered at 3 days, 2 days, and 1 day before and at 6 h after IM to the mice via gastric tube; and 3) IM + RKT, 0.2 ml of RKT (half-dose; 56.5 mg/kg or the human daily dose 113 mg/kg) were similarly orally administered at 3 days, 2 days, and 1 day (at 10:00 AM) before and at 6 h after IM. To assess the effects of RKT alone, mice were randomly assigned into 2 groups: Normal and Normal + RKT. After sacrifice, the muscle layer of the ileum was used for histochemical staining for MPO and immunohistochemical staining for macrophages. The 5-HT$_3$ receptor agonist (mCPBG: *m*-chlorophenyl-biguamide, 0.5 mg/kg, s.c.; Sigma-Aldrich, St. Louis, MO, USA) or ghrelin receptor antagonist ([D-Lys3]-

GHRP-6; 400 nmol/mouse and 1200 nmol/mouse, i.p.; Bachem, Bubendorf, Switzerland) were dissolved in physiologic saline before use and also applied 30 min before each RKT administration as necessary. Mice were euthanized at 24 h after IM. All experiments including the study regarding the effects of RKT alone was done under the fasted condition after IM. All animals recovered rapidly from the bowel manipulation procedure (within 3 days, data not shown). We therefore evaluated the efficacy of RKT at 24 h after IM. Surgery is generally performed according to plan in clinical practice, except in extreme emergencies; prophylactic administration of RKT before IM may therefore have important clinical implications.

Statistics

Results are expressed as means ± S.E.M. Data were statistically evaluated using the unpaired Student's *t*-test for comparisons between two groups and by one-way analysis of variance (ANOVA) followed by Dunnett's test for comparisons among three or more groups. Values of $P < 0.05$ were considered to be statistically significant.

Results

Three-dimensional HPLC

The HPLC profile of our handmade RKT is shown in Fig. 1. HPLC analysis revealed that the prepared RKT contained important active ingredients such as liquiritin, hesperidin, ginsenoside Rg1, glycyrrhizin, [6]-gingerol and [6]-shogaol.

Recovery of IM-induced intestinal transit disorder by treatment with RKT

The effects of RKT on delayed intestinal transit in the mouse POI model are summarized in Fig. 2. Approximately 6% of the orally administered labeled phenol red (PR) remained inside the stomach, while 94% was transported down the intestine to the distal end of the ileum, peaking at SI-8 in the normal group (Fig. 2A). The average calculated from the geometric center and gastric emptying rate in the normal group were 7.14% ± 0.15% and 94.05% ± 0.60% for the 15 segments of the gastro-intestinal tract, respectively (Fig. 2: B and C). In the IM + vehicle group, approximately 50% of the orally administered labeled PR remained inside the stomach, while 50% was transported to SI-1 and SI-2 (Fig. 2A). The IM group showed significantly delayed rates for the geometric center at 1.92 ± 0.08 and gastric emptying at 49.57 ± 4.08, as compared with the normal group (Fig. 2: B and C). The IM + RKT (113 mg/kg) group showed significant recovery of the delayed intestinal transit caused by IM, in which 12% of the orally administered
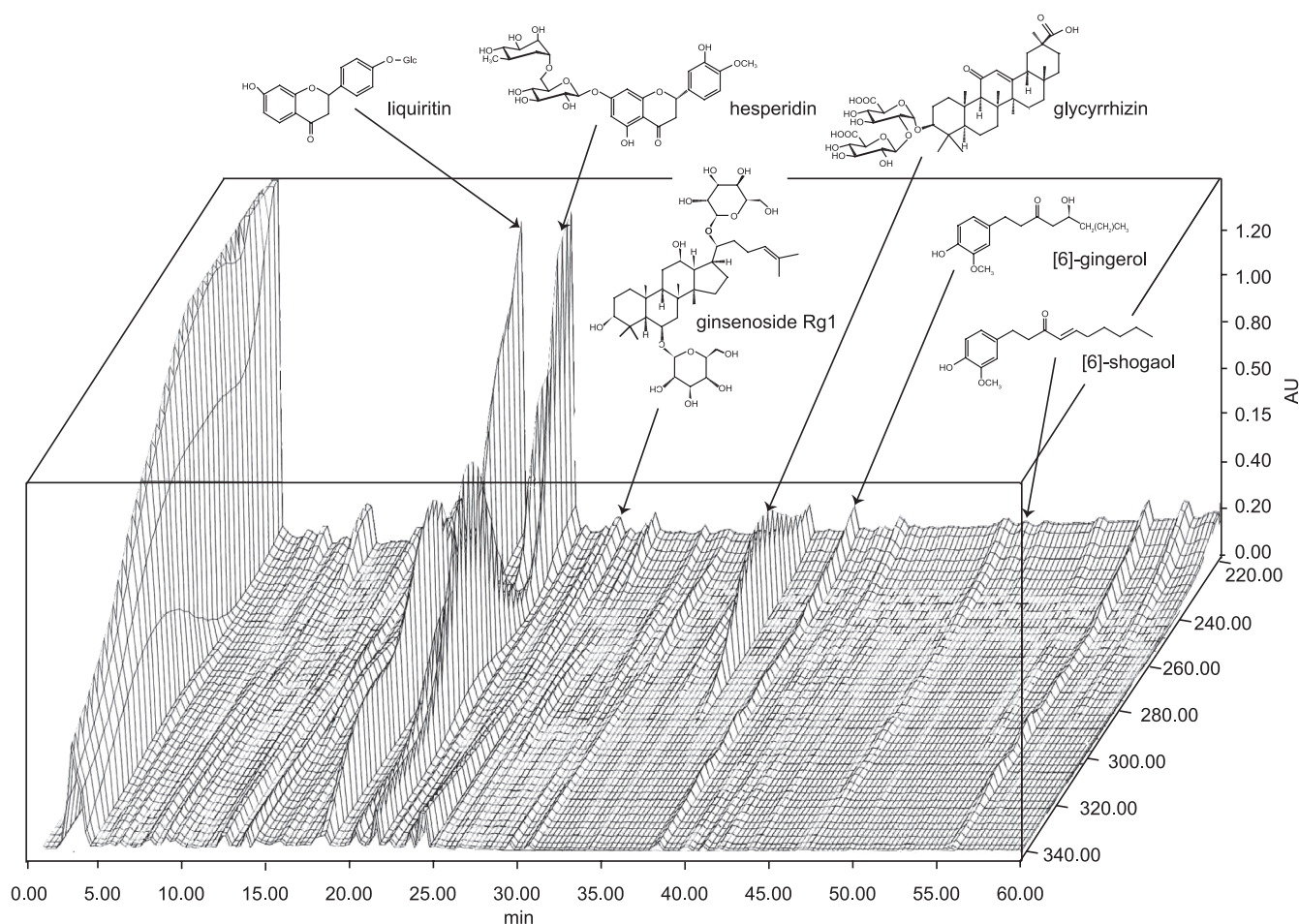
Fig. 1. HPLC profile of RKT. RKT analyzed by HPLC (ACQUITY UPLC; Nihon Waters K.K., Tokyo) under the following conditions: column, COSMOSIL C18-MS-II (3.0 × 50 mm); mobile phase, H_2O:CH_3Hn (9:1 to 1:1, linear gradient, for 95 min); flow rate; 1.0 ml/min; oven temperature, 30°C; injection volume, 10 μl.

content remained in the stomach, while 88% of the transported content moved between SI-1 and SI-3, peaking in SI-3 (Fig. 2A). Both the geometric center and gastric emptying rate in IM + RKT (113 mg/kg) were significantly higher, reaching 3.84 ± 0.38 and 88.09 ± 2.00, respectively (Fig. 2: B and C). In normal mice, RKT had no significant effect on intestinal transit and gastric emptying rate (geometric center: normal, 7.49 ± 0.22 and + RKT, 7.70 ± 0.72; Gastric emptying rate: normal, $95.38\% \pm 0.74\%$ and + RKT, $96.36\% \pm 2.57\%$, n = 3 − 5).

Effect of RKT treatment on IM-induced delayed gastric emptying measured by ^{13}C-acetate breath test

We further examined an effect of RKT on gastric emptying rate by measuring the ^{13}C-acetate breath test. Curves obtained for $^{13}CO_2$ excretion in the 2 different doses of IM + RKT, IM, and normal groups are shown in Fig. 3. Excretion (A) and cumulative excretion (B) of

$^{13}CO_2$ in the IM group were significantly lower than those in the normal group ($P < 0.01$ by ANOVA). At each time-point from 10 to 30 min, excretion of $^{13}CO_2$ in the IM group was significantly lower ($P < 0.05$ each) than those of the normal group. At each time-point from 15 to 60 min, cumulative excretion of $^{13}CO_2$ in the IM group was significantly lower than that in the normal group ($P < 0.05$ each). The maximum concentration (C max, $\Delta‰$) (Normal, 51.85 ± 7.36; IM + vehicle, 22.98 ± 1.90, $P < 0.05$) and the area under the curve (AUC, $\Delta‰$/min) (Normal, 1263.65 ± 317.20; IM + vehicle, 191.07 ± 23.08, $P < 0.05$) decreased in IM but the time to reach the maximum concentration (T max; min) (Normal, 20 ± 1.18; IM + vehicle, 25 ± 3.12) did not change significantly in IM.

Excretion of $^{13}CO_2$ in the IM + RKT (56.5 and 113 mg/kg) group significantly increased ($P < 0.05$ each, by ANOVA) compared with IM. But otherwise, RKT did not show a significant effect for C max (IM + RKT: 56.5
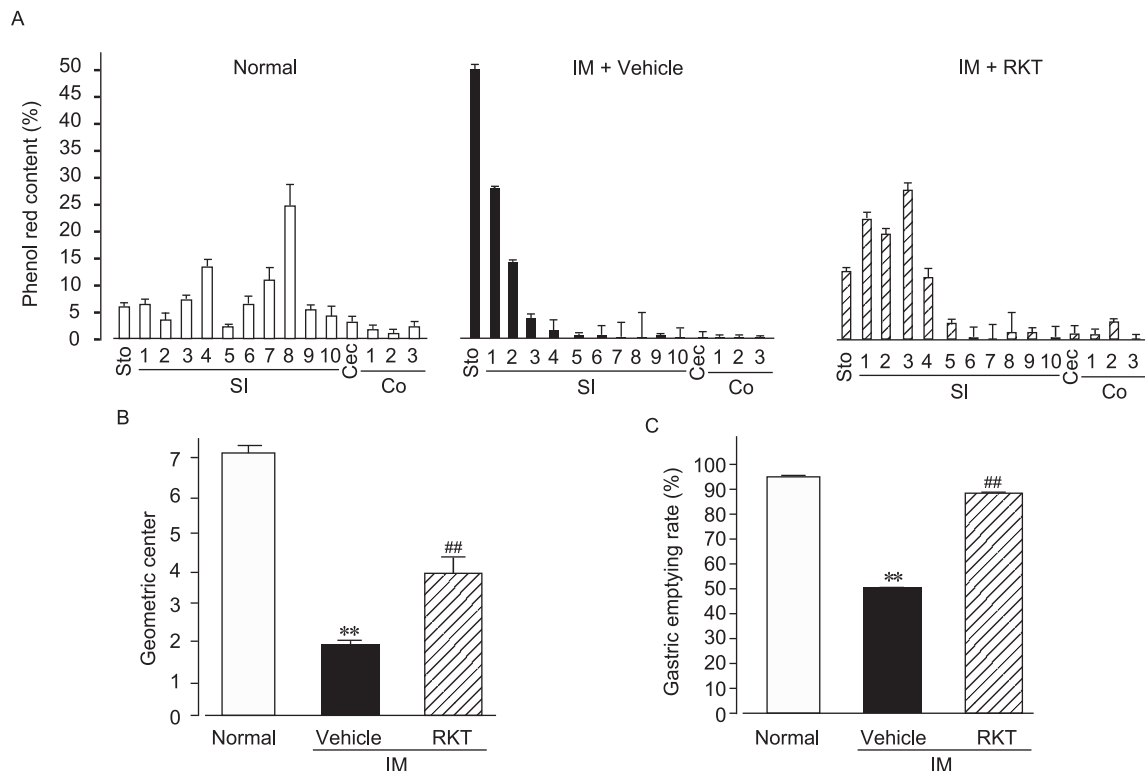
A

Fig. 2. Ameliorative action of RKT on gastrointestinal transit in mouse POI model. Detailed procedures are described in Materials and Methods. Panel A shows distribution of PR in the normal group (left graph in A), at 24 h after IM + vehicle (middle graph in A) and after IM + RKT (95 mg/kg, right graph in A). Columns indicate means ± S.E.M. for the normal group and IM + vehicle (n = 5 for each) group and IM + RKT (113 mg/kg, n = 4) group. Panels B and C show the geometric center and gastric emptying rate, as calculated from Panel A. Bars indicate means ± S.E.M. Significantly different from normal at **P < 0.01 and IM + vehicle at ##P < 0.01.

mg/kg, 36.30 ± 0.5; 113 mg/kg, 34.86 ± 2.68), AUC (56.5 mg/kg, 460.03 ± 2.19; 113 mg/kg, 496.34 ± 73.81), and T max (56.5 mg/kg, 30 ± 2.24; 113 mg/kg, 24 ± 2.0), respectively. The cumulative excretion of $^{13}CO_2$ in the IM + RKT (56.5 and 113 mg/kg) group did not change significantly.

Amelioration of IM-induced inflammation of intestinal wall by treatment with RKT

After RKT treatment, we histochemically or immuno-histochemically monitored changes in MPO-stained neutrophils or CD68-positive resident and monocyte-derived macrophages as shown in Figs. 4 and 5, respectively. In Fig. 4, MPO-stained neutrophil infiltration into the ileal muscle layer increased in the IM + vehicle group, as compared with that in the normal group. Neutrophil infiltration by IM was significantly ameliorated in the IM + RKT (113 mg/kg) group, but not in the IM + RKT (56.5 mg/kg) group. In Fig. 5, resident dendritic macrophages (20) stained by CD68 were present in the myenteric plexus region in normal intestine (18, 21). At 24 h after IM, many infiltrating monocyte-

derived macrophages and activated round (20) resident macrophages were observed, as reported previously (22). The CD68-positive macrophage population increased 6-fold in the inflamed ileal muscle layer of the intestine of the IM + vehicle group, as compared with the normal group. The increased CD68-positive macrophage population was significantly inhibited in the IM + RKT (113 mg/kg) group, as compared with the IM group; in the IM + RKT (56.5 mg/kg) group, IM-induced macrophages infiltration also tended toward ameliora-tion. RKT (113 mg/kg) had no effects on MPO-stained neutrophils or CD68-positive macrophages in the normal ileal muscle layer: MPO-positive cells (normal, 6.51 ± 1.56 cells/mm²; + RKT, 11.39 ± 3.27 cells/mm²) and CD68-positive cells (normal, 646.20 ± 14.02 cells/ mm²; + RKT, 615.20 ± 20.14 cells/mm²).

Attenuation of RKT-induced anti-inflammatory activity by mCPBG

Next, the effects of 5-HT₃ agonist mCPBG on anti-inflammatory activity of RKT in the mouse POI model are summarized in Figs. 6 and 7. As shown in Fig. 6,
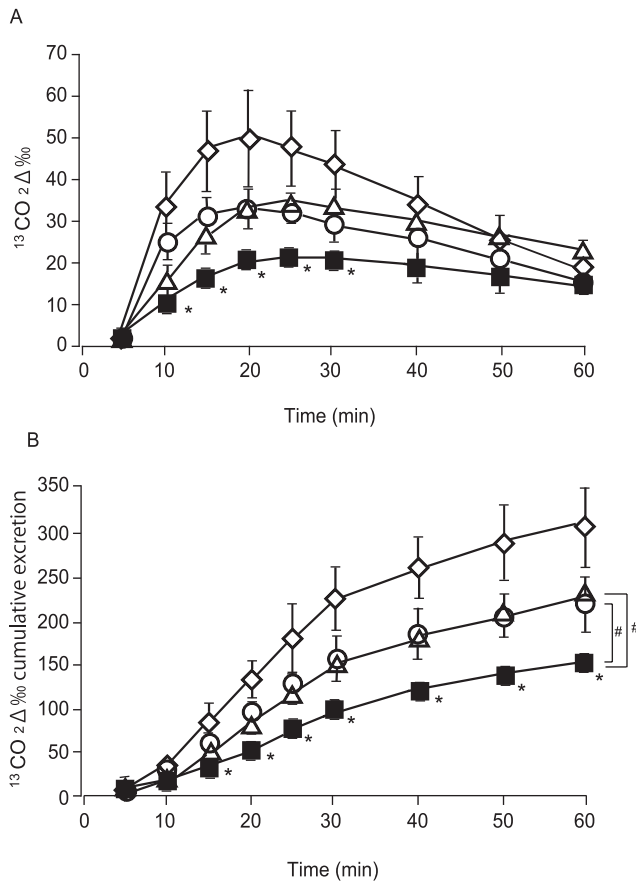
Fig. 3. Effect of RKT on excretion and cumulative excretion of $^{13}CO_2$, as calculated by the ^{13}C-acetate breath test in POI model mice. Graphs A and B show excretion and cumulative excretion curves for $^{13}CO_2$, respectively. Detailed procedures are described in Material and Methods. Open diamonds, closed squares, open triangles, and open circles indicate normal, 24 h after IM, IM with 95 mg/kg RKT, and IM with 113 mg/kg RKT groups, respectively. Each symbol indicates the mean ± S.E.M. of 4 – 5 experiments. Significantly different from normal and IM + vehicle at *P < 0.01 and #P < 0.05, respectively.

Fig. 4. Ameliorative effects of RKT on MPO-stained neutrophil infiltration in IM. Panel A indicates representative results for whole mount histochemical staining of the myenteric plexus region to detect MPO-positive neutrophils. Panel B shows quantification of neutrophil cells in the IM + RKT (56.5 and 113 mg/kg, n = 5 for each) group, normal group (n = 6), IM + vehicle group (n = 8). Each column indicates the mean ± S.E.M. Significantly different from normal and IM + vehicle at **P < 0.01 and #P < 0.05, respectively.

mCPBG treatment did not affect the ameliorative effect of RKT against IM as assessed by neutrophil infiltration. In contrast, mCPBG partially reduced the ameliorative action of RKT as assessed by macrophage infiltration, as shown in Fig. 7. We also confirmed that mCPBG itself had no effect on MPO activity and leukocyte infiltrations at the concentrations used in this study (0.0125 mg/kg, s.c.) in normal mice: MPO activity (normal, n = 4, 7.51 ± 1.58 U/g wet tissue; + mCPBG, n = 3, 21.35 ± 8.45 U/g wet tissue), MPO-positive cells (normal, 12.89 ± 1.52 cells/mm^2; + mCPBG, 21.66 ± 2.18 cells/mm^2), and CD68-positive cells (normal, 379.232 ± 30.36 cells/mm^2; + mCPBG, 251.74 ± 16.36 cells/mm^2). In addition, mCPBG did not contribute to increase inflammation by IM, as assessed by MPO activity and leukocyte infiltrations at the concentrations
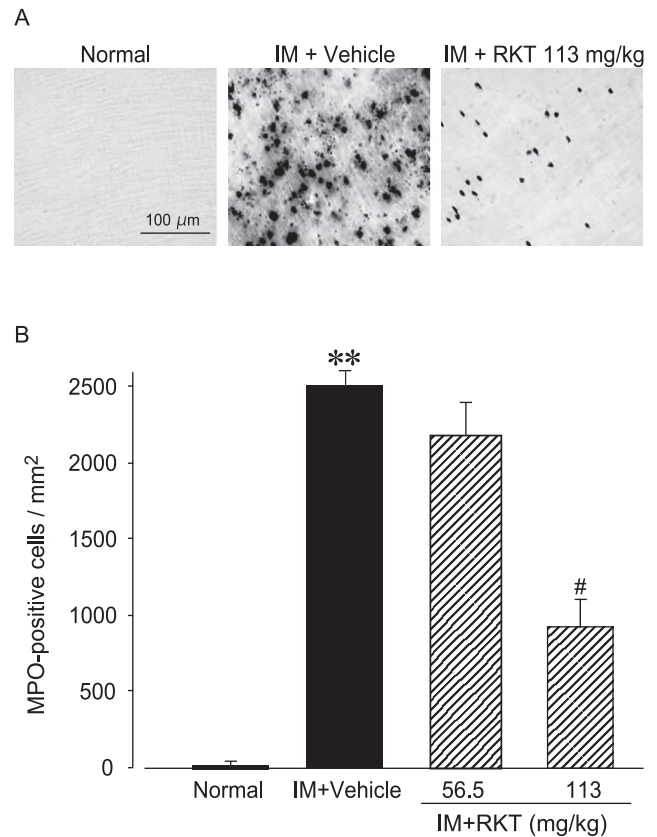
used in this study: MPO activity (normal, n = 3, 21.66 ± 1.58 U/g wet tissue; IM, 243.24 ± 10.71 U/g wet tissue; IM + mCPBG, 175.02 ± 27.61 U/g wet tissue), MPO-positive cells (normal, 7.97 ± 1.30 cells/mm^2; IM, 2742.62 ± 176.97 cells/mm^2; IM + mCPBG, 2956.87 ± 132.86 cells/mm^2), CD68-positive cells (normal, 454.92 ± 24.11 cells/mm^2; IM, 3897.57 ± 51.34 cells/mm^2; IM + mCPBG 3030.60 ± 97.41). We did not examine higher concentration of mCPBG on anti-inflammatory activity of RKT in the mouse POI model because of the inflammatory action of mCPBG itself.

Attenuation of RKT-induced anti-inflammatory activity by [D-Lys3]-GHRP-6

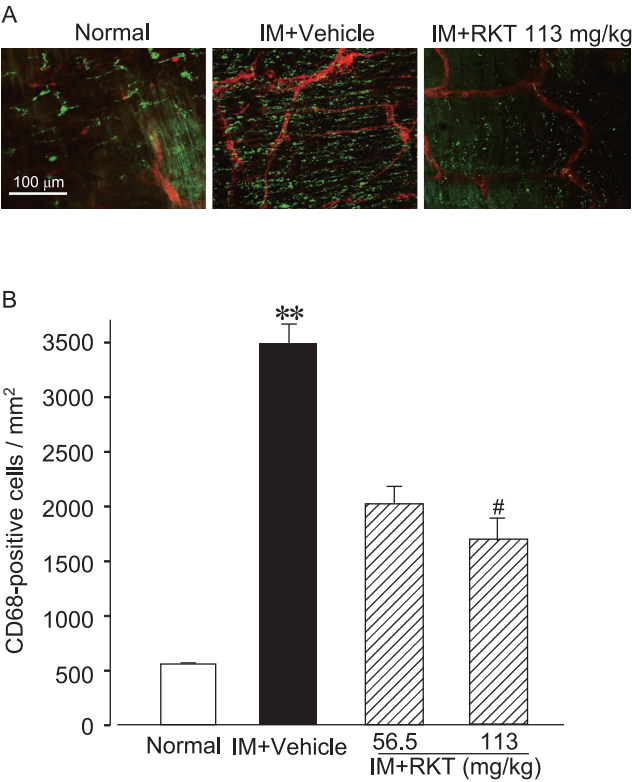The effects of [D-Lys3]-GHRP-6 on anti-inflammatory activity of RKT in the mouse POI model are summarized

Fig. 5. Ameliorative effects of RKT on CD68-positive macrophage infiltration in IM. Panel A indicates representative results for whole mount immunohistochemical staining of the myenteric plexus region to detect CD68-positive macrophages. Panel B shows quantification of macrophage cells in IM + RKT (56.5 and 113 mg/kg, n = 5 for each) group, normal (n = 6), IM + vehicle group (n = 8). Each column indicates the mean ± S.E.M. Significantly different from normal and IM + vehicle at $**P < 0.01$ and $\#P < 0.05$, respectively. Position of the myenteric plexus region was confirmed by staining with protein gene product 9.5, which detects the myenteric nerve plexus. Red signals indicate PGP9.5-positive myenteric nerves. Green signals indicate CD68-positive macrophages.

in Figs. 8 and 9. As shown in Fig. 8, [D-Lys3]-GHRP-6 significantly attenuated anti-inflammatory activity by RKT, as measured by MPO-positive neutrophil numbers (IM, 2290.08 ± 0.20; IM + RKT, 1027.43 ± 124.71; IM + RKT + [D-Lys3]-GHRP-6, 2363.92 ± 333.68, n = 4 each). [D-Lys3]-GHRP-6 gave similar results to anti-inflammatory activity by RKT, as monitored by numbers of CD-68 positive macrophages. As shown in Fig. 9, [D-Lys3]-GHRP-6 significantly attenuated the RKT-induced inhibition of macrophage infiltration by IM (IM, 1401.475 ± 146.71; IM + RKT, 836.28 ± 67.00; IM + RKT + [D-Lys3]-GHRP-6, 1771.72 ± 270.97, n = 4 each).

We confirmed that [D-Lys3]-GHRP-6 itself had no effect on MPO activity, the histochemical or immuno-histochemical properties of neutrophils, or CD68-positive macrophages in normal and IM-treated mice: MPO-positive cells (normal, 8.07 ± 0.90 cells/mm²; normal + [D-Lys3]-GHRP-6, 12.56 ± 1.43 cells/mm²; IM, 3342.193 ± 158.311 cells/mm²; IM + [D-Lys3]-GHRP-6, 3177.191 ± 126.88) and CD68-positive cells (normal, 797.21 ± 27.10 cells/mm²; + [D-Lys3]-GHRP-6, 859.09 ± 22.77 cells/mm²; IM, 3902.66 ± 135.07 cells/mm²; IM + [D-Lys3]-GHRP-6, 2908.41 ± 134.43).

Attenuation of RKT-induced recovery of intestinal transit by [D-Lys3]-GHRP-6

Approximately 7% of the orally administered labeled phenol red (PR) remained inside the stomach, while 93% was transported down the intestine to the distal end of the ileum, peaking at SI-8 in the normal group (Fig. 10A). The average calculated from the geometric center and gastric emptying rate in the normal group were 7.38% ± 0.15% and 93.16% ± 0.69%, respectively (Fig. 10: B and C). In the IM + vehicle group, approximately 17% of the orally administered labeled PR remained inside the stomach, while 83% was transported to SI-7 (Fig. 10A). The IM group showed significantly
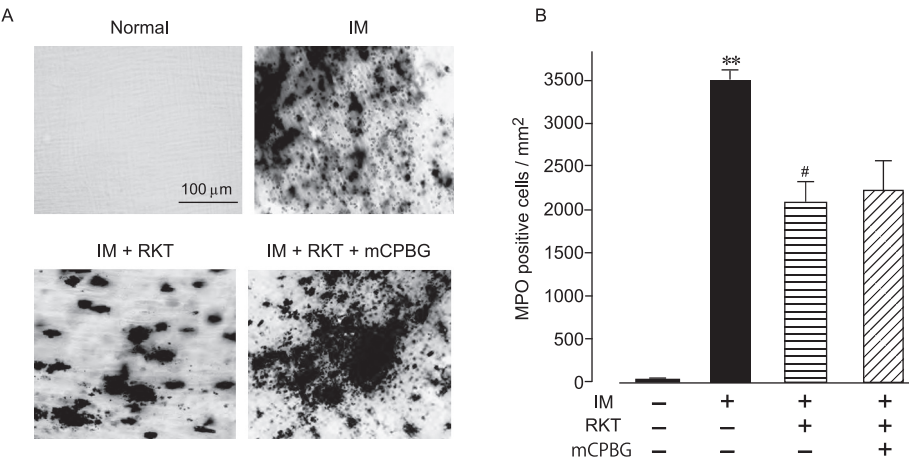

Fig. 6. Ameliorative effects of RKT and negative effects of mCPBG on MPO-positive neutrophil infiltration in mouse POI model. Panels A and B show representative images of MPO-positive neutrophil infiltration into the myenteric plexus region and quantification results. Columns indicate the mean ± S.E.M. from normal and IM + vehicle group (n = 5 for each), IM + RKT + mCPBG group (n = 4). Significantly different from normal and IM + vehicle at $**P < 0.01$ and $\#P < 0.05$, respectively.
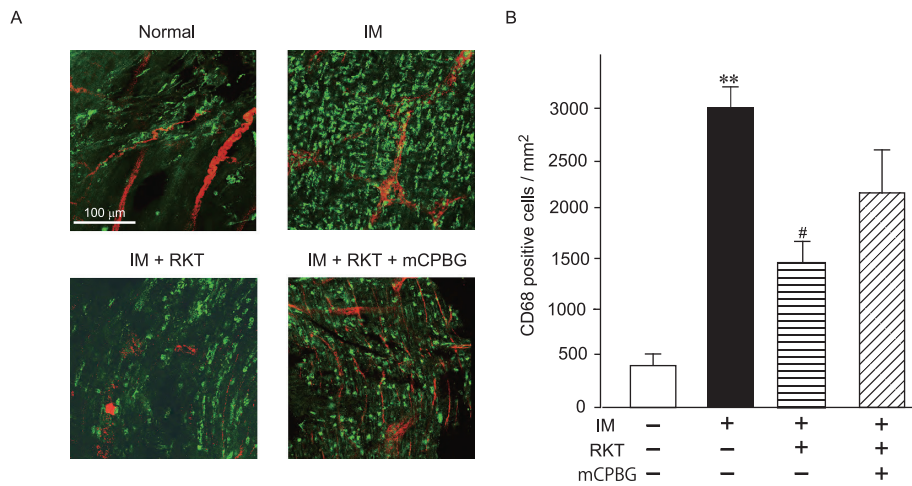
A

Normal

IM

IM + RKT

IM + RKT + mCPBG

100 μm

B

Fig. 7. Ameliorative effects of RKT and negative effects of mCPBG on CD68-positive macrophage infiltration in mouse POI model. A and B show representative images of MPO-positive macrophage infiltration into the myenteric plexus region and quantification results. Each column indicates the mean ± S.E.M. from normal and IM + vehicle group (n = 5 for each) and IM + RKT + mCPBG group (n = 4). Significantly different from normal and IM + vehicle at **$P < 0.01$ and #$P < 0.05$, respectively.

A

Normal

IM

IM + RKT

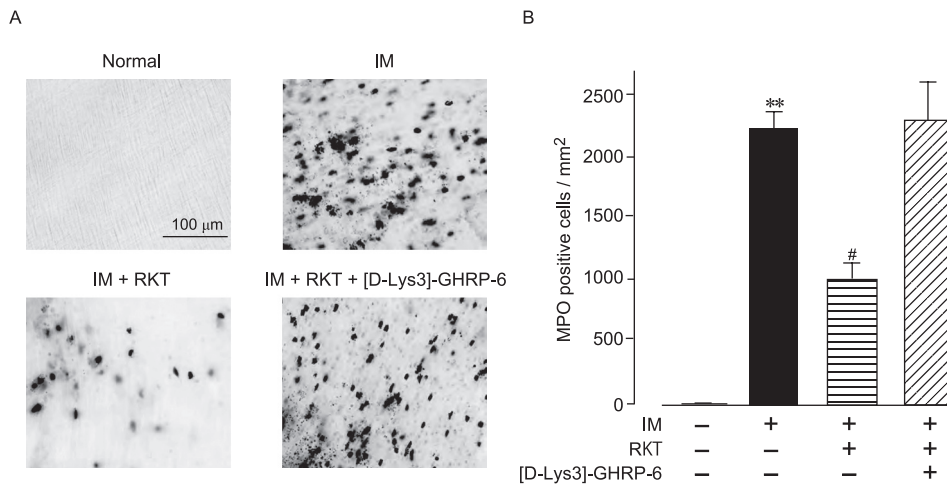IM + RKT + [D-Lys3]-GHRP-6

100 μm

B

Fig. 8. Ameliorative effects of RKT and negative effects of [D-Lys3]-GHRP-6 on MPO-positive neutrophil infiltration in mouse POI model. Panels A and B show representative images of MPO-positive neutrophil infiltration into the myenteric plexus region and quantification results. Each column indicates the mean ± S.E.M. from n = 4/group. Significantly different from normal and IM + vehicle at **$P < 0.01$ and #$P < 0.05$, respectively.

A

Normal

IM

IM + RKT
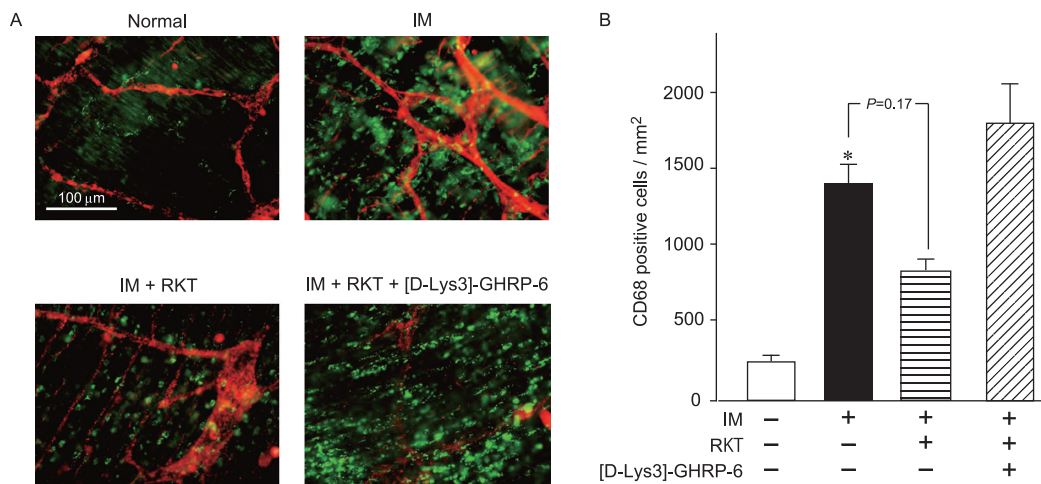
IM + RKT + [D-Lys3]-GHRP-6

100 μm

B

Fig. 9. Ameliorative effects of RKT and negative effects of [D-Lys3]-GHRP-6 on CD68-positive macrophage infiltration in mouse POI model. Panels A and B show representative images of MPO-positive macrophage infiltration into the myenteric plexus region and quantification results. Each column indicates the mean ± S.E.M. from n = 4/group. Significantly different from normal at *$P < 0.05$.

delayed rates for the geometric center at 5.63 ± 0.35 and gastric emptying at $83.46\% \pm 5.23\%$, as compared with the normal group (Fig. 10: B and C). The IM + RKT (113 mg/kg) group showed significant recovery of the delayed intestinal transit caused by IM, in which 17% of the orally administered content remained in the stomach, while 83% of the transported content moved between SI-4 and SI-9, peaking in SI-4 (Fig. 10A). Both the geometric center and gastric emptying rate in IM + RKT (113 mg/kg) were higher, reaching $7.09\% \pm 0.22\%$ and $96.01\% \pm 0.39\%$, respectively (Fig. 10: B and C). The group pretreated with mCPBG before RKT administration showed no reduction in the ameliorative effect of RKT against IM. In contrast, groups pretreated with [D-Lys3]-GHRP-6 (400 and 1200 nmol) showed partial reduction of the ameliorative action of RKT, in which 6% (400 nmol group) and 20% (1200 nmol group) of the orally administered PR content remained in the stomach, while 96% (400 nmol group) and 80% (1200 nmol group) of the transported PR content moved between SI-3 and SI6, peaking in SI-5 (400 nmol group)

and between SI-2 and SI-8, peaking in SI-2 (1200 nmol group), respectively (Fig. 10A). Both the geometric center and gastric emptying rate in IM + RKT + [D-Lys3]-GHRP-6 (400 and 1200 nmol) showed trends of partial reduction, reaching $6.00\% \pm 0.17\%$ and $94.03\% \pm 1.08\%$ (400 nmol group) and $5.79\% \pm 0.27\%$ and $80.00\% \pm 5.93\%$, respectively (Fig. 10: B and C).

Discussion

Several studies reported that RKT shows a prokinetic effect mainly in the upper gastrointestinal tract (2, 23 – 26), and we have confirmed that RKT significantly recovered the delayed gastric emptying and intestinal transit dysfunction induced by IM in the mouse POI model. In addition, we further showed for the first time that RKT significantly suppresses neutrophil and macrophage infiltrations induced by IM, suggesting that RKT produces an anti-inflammatory effect in POI. These findings might indicate the possibility that RKT clinically ameliorates POI through improvements in both
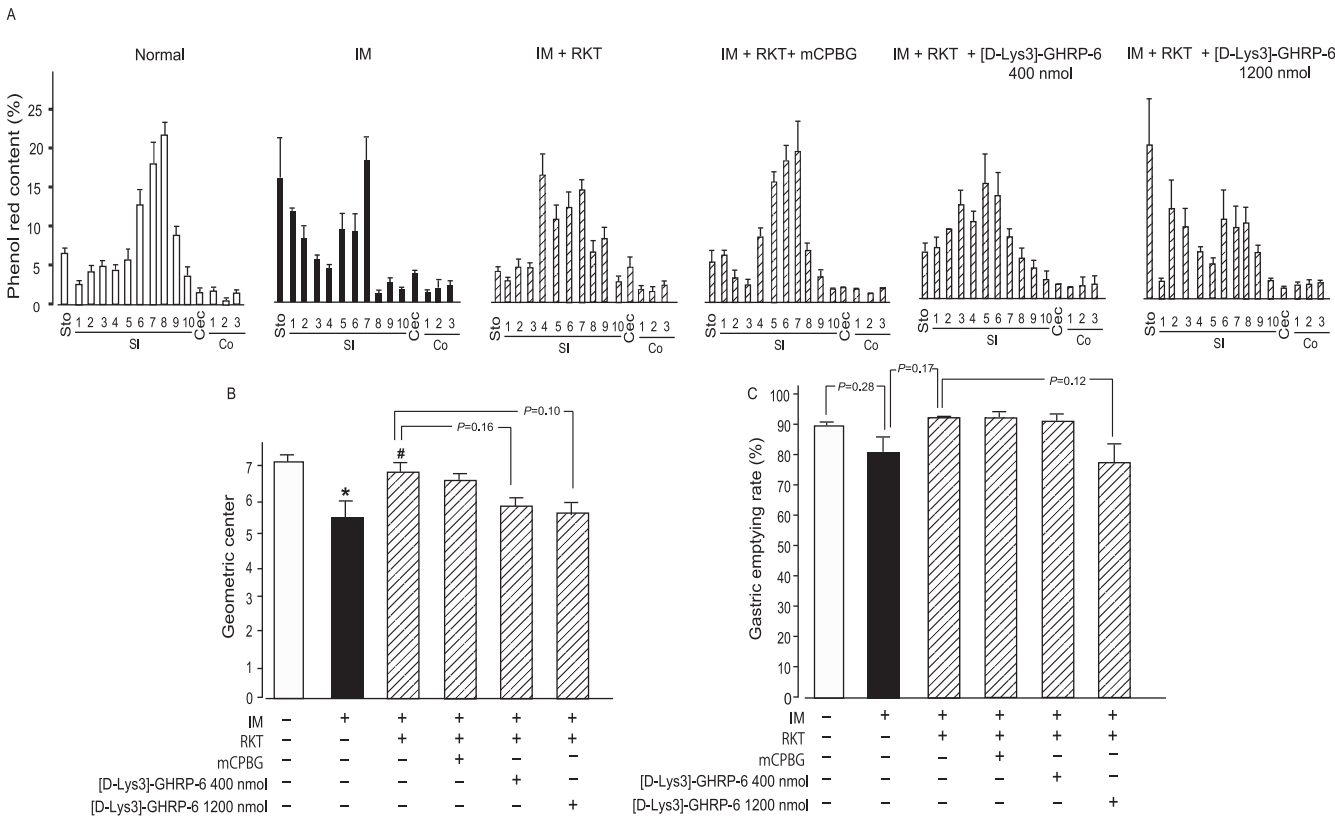

Fig. 10. Effects of mCPBG and [D-Lys3]-GHRP-6 on ameliorative effects of RKT in mouse POI model as assessed by gastrointestinal transit. In this experimental condition, we performed weaker IM treatment rather than that in Fig. 2 to detect effects of mCPBG and [D-Lys3]-GHRP-6 easily, so the geometric center value of IM-treated mice was higher. Columns indicate means ± S.E.M. of n = 4/group. Panels B and C show the geometric center and gastric emptying rate, as calculated from panel A. Bars indicate means ± S.E.M. Significantly different from normal and IM + vehicle at *$P < 0.05$ and #$P < 0.05$, respectively.

gastrointestinal motility and inflammation.

Until now, several mechanisms for the gastroprokinetic action of RKT have been reported. RKT increases gastric emptying by the 5-HT$_3$ receptor antagonism in rats (2). Efficacy of RKT was reported to be comparable to the 5-HT$_3$ antagonist ondansetron. Another mechanism may be mediated by ghrelin. Abdominal surgery induces a rapid and long-lasting reduction of circulating levels of acyl ghrelin (4). Besides modulation of appetite, ghrelin and ghrelin-receptor agonist have recently been reported to stimulate gastric, small intestinal, and colorectal motility, by increasing gastric tone and emptying, increasing activity of migration motor complexes in the small bowel, and activation of the spinal cord. (5 – 7, 27 – 29) Our observation suggests that efficacy of RKT appears to be significant but relatively weak on the delayed gastric emptying by IM, as monitored with the ^{13}C-acetate breath test, but delayed gastric emptying rate monitored by intestinal transit test was more apparently recovered by RKT. Moreover, intestinal transit study also revealed that RKT facilitates the lower intestinal tract, suggesting that RKT might be applicable for the treatment of intestinal motility disorder mediated through POI.

Recent studies revealed that 5-HT$_3$ receptor antagonists, granisetron and tropisetron, ameliorate acetic acid–induced colitis in rats as indicated by improved macroscopic and histological features, correction of the elevated amounts of biochemical markers MPO and malondialdehyde, an index of lipid peroxidation. Granisetron and tropisetron also decreased colonic content of inflammatory cytokines (30, 31). The anti-inflammatory effects of granisetron were canceled by concurrent administration of mCPBG (30). This data suggests that the improvement effects of granisetron in acetic acid-induced colitis could be mediated by 5-HT$_3$ receptors (30). Furthermore, ghrelin has also been reported to have anti-inflammatory effect on trinitro-benzene sulfonic acid or DSS-induced colitis in the mouse as a potent immunomodulatory factor capable of deactivating the intestinal inflammatory response and restoring mucosal immune tolerance at multiple levels (8). These findings led us to an idea that RKT is a novel source of drug for POI as well as other inflammatory gastrointestinal diseases because RKT is known to be a 5-HT$_3$ receptor antagonist and enhancer of ghrelin secretion. Actually, a clinical trial has been undertaken for the treatment of POI using ghrelin agonists (32, 33). We therefore examined whether both 5-HT$_3$ receptor antagonistic action and ghrelin suppression of RKT are related to the anti-inflammatory action, using 5-HT$_3$ receptor agonist mCPBG and ghrelin antagonist [D-Lys3]-GHRP-6. Results indicated that [D-Lys3]-GHRP-6

significantly inhibited the RKT-mediated anti-inflammatory activity, as monitored by infiltrating macrophages and neutrophils. On the other hand, mCPBG treatment did not affect the ameliorative effect of RKT against IM as assessed by neutrophil infiltration. In contrast, mCPBG partially reduced the ameliorative action of RKT as assessed by macrophage infiltration. These results suggest that RKT-induced anti-inflammatory action in the mouse POI model may be mediated through both 5-HT$_3$ receptor inhibition and ghrelin release. [D-Lys3]-GHRP-6 showed trends of partial attenuation of the ameliorative action of RKT against delayed gastrointestinal transit by IM, which is compatible with our data on amelioration of inflammation induced by RKT. On the other hand, mCPBG did not affect the ameliorative effect of RKT against IM as assessed by intestinal transit. Over 1 mg/kg (4 mg/body) mCPBG induced neutrophil infiltrations into the muscle layer of the small intestine, which may be an inflammatory action of mCPBG alone (data not shown , n = 3).

It was reported that the herb *Aurantii nobilis pericarpium* includes target component flavonoids HMF, hesperidin, and isoliquiritigenin in RKT (3). These flavonoids also induce prokinetic ability through improvement of ghrelin release owing to the 5-HT$_{2B}$ and 5-HT$_{2C}$ receptor antagonistic action (3). Moreover it was demonstrated that hesperidin showed pharmacological efficacy in enhancing gastric motility via antagonism of a 5-HT$_3$ receptor–associated pathway (2). These flavonoids and herbs may have multiple actions including anti-inflammatory ability. Further studies are needed to elucidate rather complicated action mechanisms of herbal medicine, which could include many kinds of unknown but profitable ingredients.

In conclusion, RKT may serve as a new therapeutic agent against POI, as characterized by its anti-inflammatory potency, in addition to its gastrointestinal prokinetic action. Our findings may widen range of clinical applications of RKT in gastrointestinal diseases.

Acknowledgments

Conflicts of Interest

No conflicts of interest, financial or otherwise, are declared by the authors.

References

1 Kusunoki H, Haruma K, Hata J, Ishii M, Kamada T, Yamashita N, et al. Efficacy of Rikkunshito, a traditional Japanese medicine (Kampo), in treating functional dyspepsia. Intern Med. 2010;49: 2195–2202.

2 Tominaga K, Kido T, Ochi M, Sadakane C, Mase A, Okazaki H, et al. The traditional Japanese medicine Rikkunshito promotes gastric emptying via the antagonistic action of the 5-HT$_3$ receptor pathway in rats. Evid Based Complement Alternat Med. 2011; 2011:248481.

3 Takeda H, Sadakane C, Hattori T, Katsurada T, Ohkawara T, Nagai K, et al. Rikkunshito, an herbal medicine, suppresses cisplatin-induced anorexia in rats via 5-HT$_2$ receptor antagonism. Gastroenterology. 2008;134:2004–2013.

4 Stengel A, Goebel-Stengel M, Wang L, Shaikh A, Lambrecht NW, Rivier J, et al. Abdominal surgery inhibits circulating acyl ghrelin and ghrelin-O-acyltransferase levels in rats: role of the somatostatin receptor subtype 2. Am J Physiol Gastrointest Liver Physiol. 2011;301:G239–G248.

5 Camilleri M, Papathanasopoulos A, Odunsi ST. Actions and therapeutic pathways of ghrelin for gastrointestinal disorders. Nat Rev Gastroenterol Hepatol. 2009;6:343–352.

6 Mondal A, Xie Z, Miyano Y, Tsutsui C, Sakata I, Kawamoto Y, et al. Coordination of motilin and ghrelin regulates the migrating motor complex of gastrointestinal motility in Suncus murinus. Am J Physiol Gastrointest Liver Physiol. 2012;302:G1207–G1215.

7 Murray CD, Martin NM, Patterson M, Taylor SA, Ghatei MA, Kamm MA, et al. Ghrelin enhances gastric emptying in diabetic gastroparesis: a double blind, placebo controlled, crossover study. Gut. 2005;54:1693–1698.

8 Gonzalez-Rey E, Chorny A, Delgado M. Therapeutic action of ghrelin in a mouse model of colitis. Gastroenterology. 2006; 130:1707–1720.

9 Pamukcu O, Kumral ZN, Ercan F, Yegen BC, Ertem D. Anti-inflammatory effect of obestatin and ghrelin in dss-induced colitis in rats. J Pediatr Gastroenterol Nutr. 2013;57:211–218.

10 Wehner S, Behrendt FF, Lyutenski BN, Lysson M, Bauer AJ, Hirner A, et al. Inhibition of macrophage function prevents intestinal inflammation and postoperative ileus in rodents. Gut. 2007;56:176–185.

11 Kalff JC, Carlos TM, Schraut WH, Billiar TR, Simmons RL, Bauer AJ. Surgically induced leukocytic infiltrates within the rat intestinal muscularis mediate postoperative ileus. Gastroenterology. 1999;117:378–387.

12 Bauer AJ, Boeckxstaens GE. Mechanisms of postoperative ileus. Neurogastroenterol Motil. 2004;16 Suppl 2:54–60.

13 Schmidt J, Stoffels B, Moore BA, Chanthaphavong RS, Mazie AR, Buchholz BM, et al. Proinflammatory role of leukocyte-derived Egr-1 in the development of murine postoperative ileus. Gastroenterology. 2008;135:926–936.

14 Schwarz NT, Kalff JC, Turler A, Engel BM, Watkins SC, Billiar TR, et al. Prostanoid production via COX-2 as a causative mechanism of rodent postoperative ileus. Gastroenterology. 2001;121:1354–1371.

15 Uchida M, Endo N, Shimizu K. Simple and noninvasive breath test using ^{13}C-acetic acid to evaluate gastric emptying in conscious rats and its validation by metoclopramide. J Pharmacol Sci. 2005;98:388–395.

16 Hoshino T, Oikawa T, Endo M, Hanawa T. The utility of noninvasive ^{13}C-acetate breath test using a new solid test meal to measure gastric emptying in mice. J Smooth Muscle Res. 2008;44:159–165.

17 Kinoshita K, Horiguchi K, Fujisawa M, Kobirumaki F, Yamato S, Hori M, et al. Possible involvement of muscularis resident macrophages in impairment of interstitial cells of Cajal and myenteric nerve systems in rat models of TNBS-induced colitis. Histochem Cell Biol. 2007;127:41–53.

18 Hori M, Kita M, Torihashi S, Miyamoto S, Won KJ, Sato K, et al. Upregulation of iNOS by COX-2 in muscularis resident macrophage of rat intestine stimulated with LPS. Am J Physiol Gastrointest Liver Physiol. 2001;280:G930–G938.

19 Sheibani K, Lucas FV, Tubbs RR, Savage RA, Hoeltge GA. Alternate chromogens as substitutes for benzidine for myeloperoxidase cytochemistry. Am J Clin Pathol. 1981;75:367–370.

20 Hori M, Nobe H, Horiguchi K, Ozaki H. MCP-1 targeting inhibits muscularis macrophage recruitment and intestinal smooth muscle dysfunction in colonic inflammation. Am J Physiol Cell Physiol. 2008;294:C391–C401.

21 Mikkelsen HB, Thuneberg L, Rumessen JJ, Thorball N. Macrophage-like cells in the muscularis externa of mouse small intestine. Anat Rec. 1985;213:77–86.

22 Tsuchida Y, Hatao F, Fujisawa M, Murata T, Kaminishi M, Seto Y, et al. Neuronal stimulation with 5-hydroxytryptamine 4 receptor induces anti-inflammatory actions via alpha7nACh receptors on muscularis macrophages associated with postoperative ileus. Gut. 2011;60:638–647.

23 Furukawa N, Manabe N, Kase Y, Hattori T, Imamura H, Kusunoki H, et al. Intragastric infusion of rikkunshito (kampo) induces proximal stomach relaxation in conscious dogs. Auton Neurosci. 2013;179:14–22.

24 Yanai M, Mochiki E, Ogawa A, Morita H, Toyomasu Y, Ogata K, et al. Intragastric administration of rikkunshito stimulates upper gastrointestinal motility and gastric emptying in conscious dogs. J Gastroenterol. 2013;48:611–619.

25 Shiratori M, Shoji T, Kanazawa M, Hongo M, Fukudo S. Effect of rikkunshito on gastric sensorimotor function under distention. Neurogastroenterol Motil. 2011;23:323–329.

26 Kawahara H, Kubota A, Hasegawa T, Okuyama H, Ueno T, Ida S, et al. Effects of rikkunshito on the clinical symptoms and esophageal acid exposure in children with symptomatic gastroesophageal reflux. Pediatr Surg Int. 2007;23:1001–1005.

27 Masuda Y, Tanaka T, Inomata N, Ohnuma N, Tanaka S, Itoh Z, et al. Ghrelin stimulates gastric acid secretion and motility in rats. Biochem Biophys Res Commun. 2000;276:905–908.

28 Fujino K, Inui A, Asakawa A, Kihara N, Fujimura M, Fujimiya M. Ghrelin induces fasted motor activity of the gastrointestinal tract in conscious fed rats. J Physiol. 2003;550:227–240.

29 Shimizu Y, Chang EC, Shafton AD, Ferens DM, Sanger GJ, Witherington J, et al. Evidence that stimulation of ghrelin receptors in the spinal cord initiates propulsive activity in the colon of the rat. J Physiol. 2006;576:329–338.

30 Fakhfouri G, Rahimian R, Daneshmand A, Bahremand A, Rasouli MR, Dehpour AR, et al. Granisetron ameliorates acetic acid-induced colitis in rats. Hum Exp Toxicol. 2010;29: 321–328.

31 Mousavizadeh K, Rahimian R, Fakhfouri G, Aslani FS, Ghafourifar P. Anti-inflammatory effects of 5-HT receptor antagonist, tropisetron on experimental colitis in rats. Eur J

Clin Invest. 2009;39:375–383.

32 Bochicchio G, Charlton P, Pezzullo JC, Kosutic G, Senagore A. Ghrelin agonist TZP-101/ulimorelin accelerates gastrointestinal recovery independently of opioid use and surgery type: covariate analysis of phase 2 data. World J Surg. 2012;36:39–45.

33 Popescu I, Fleshner PR, Pezzullo JC, Charlton PA, Kosutic G, Senagore AJ. The Ghrelin agonist TZP-101 for management of postoperative ileus after partial colectomy: a randomized, dose-ranging, placebo-controlled clinical trial. Dis Colon Rectum. 2010;53:126–134.